the energy absorbed by the waveguide material were plotted for a case in which the waveguide radius was varied from 100 to 500 mm and all other parameters were kept constant. The collection efficiencies from the two were within 1.5 % of each other and the energy collected values were almost same. The energy absorbed values predicted by the analytical model is higher than that being predicted in the simulations and that is because a few loss mechanisms like the energy lost due to reflection at the surfaces and absorption in the lens array is ignored to simplify the model. The over estimation of the energy absorbed by the waveguide material leads to safer design in terms of thermal stress and temperature limitations. This analytical model has been used for the parametric study and the design studies which will be discussed in this section.

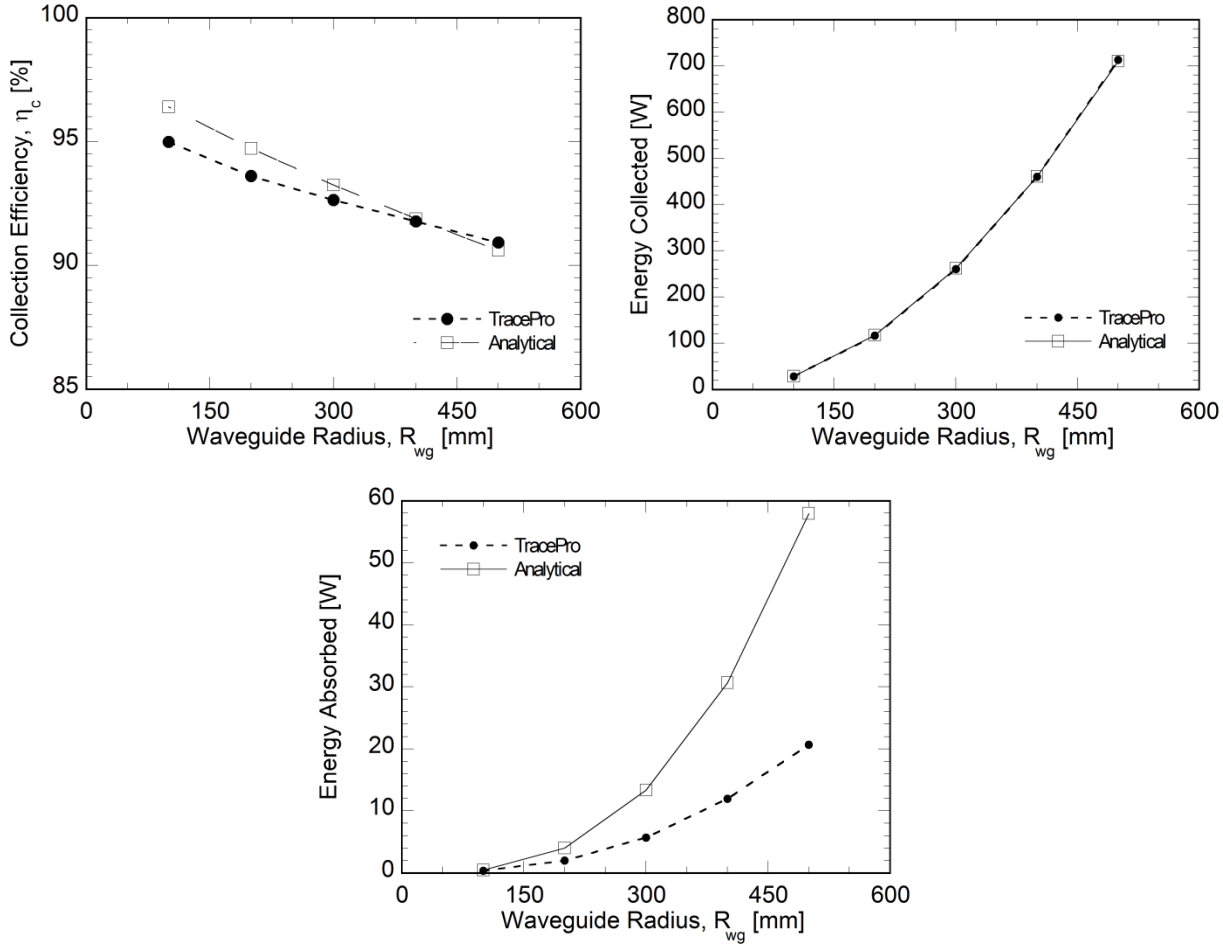

Figure 19. Validation of the analytical model by plotting the variation of collection efficiency, energy collected and energy absorbed with waveguide radius from the analytical model and the TracePro simulations

Figure 20 shows the spatial variation of the Temperature rise, ΔT for the different convective heat transfer coefficients, radius of waveguide, and thickness of waveguide and incident irradiation.

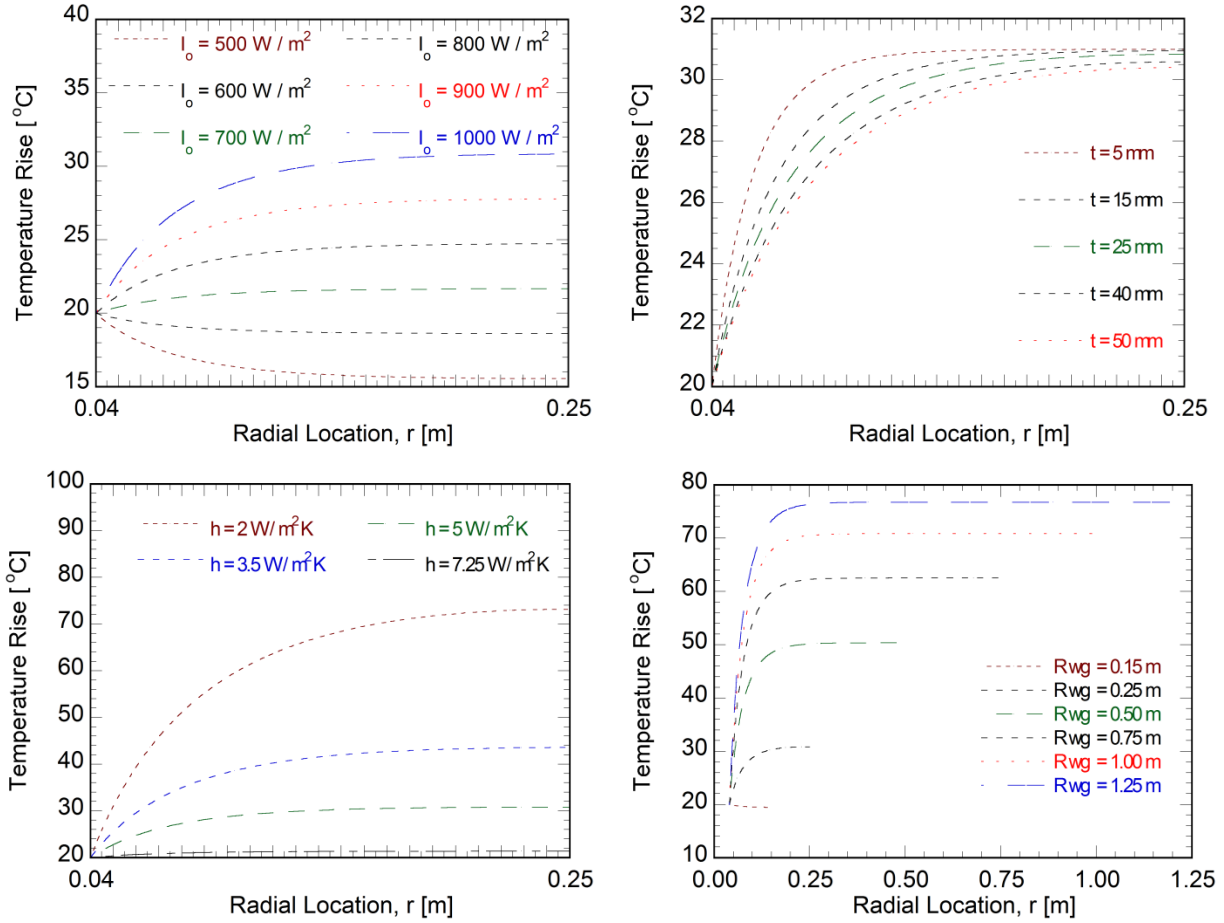

Figure 20. Influence of incident irradiance, waveguide thickness, convective heat transfer coefficient and waveguide radius on the spatial distribution of temperature rise within the radial waveguide

The temperature increases from the center of the waveguide to the ends and reaches a maximum value for a given set of parameters asymptotically. This is true in the case of low temperature applications in which the receiver temperature is kept at 50 ^{0}C. The cases in which the intensity of the incident irradiation is low, the temperature is highest at the central receiver and decreases towards the ends and stabilizes to a minimum temperature. This can be seen in the case where the irradiation is 500 W/m^2 and 600 W/m^2. In these cases, the effect of convective cooling over power the effect of energy absorption by the waveguide. The temperature rise is

less in case of thicker waveguides as the heat capacity of the waveguide increases because of the higher volume. The temperature rise is also dependent on the convective heat transfer coefficient and as the convective heat transfer coefficient is increased, the temperature rise decreases. In larger waveguides, even though the total incident irradiation is higher, its effect on the temperature rise is counteracted by the increase in heat capacity of the waveguide. The amount of energy absorbed the waveguide increases in larger waveguides due to the fact that the rays have to travel longer through the waveguide material to reach the absorbing surface. This leads to higher temperature rise in larger waveguides when compared to smaller waveguides.

Figure 21a shows the net thermal power delivered (P_t) to the receiver as a function of radius for various incident solar irradiation for low temperature applications ($T_F = 100\,℃$). The thickness of waveguide is kept constant at 10 mm. As expected, P_t increases with increase in incident solar irradiation. The trade-off between the exponential decay in totally internally reflected irradiation due to absorption and the increase in total incident irradiation with increase in radius results in the net delivered thermal power to increase asymptotically in Figure 21a.

Figure 21b shows the required aperture area per unit thermal power delivered (A), which is the ratio of waveguide area and net thermal power delivered (P_t). The required aperture increases with increase in radius due to increased absorption loss of the solar irradiation within the waveguide, despite the increase in collection area, which is also inferred from the asymptotic increase in P_t in Fig. 21a. Therefore, there exists a maximum desired waveguide radius based on the asymptotic increase in P_t and increase in aperture area (A). For constant radius, aperture requirement reduces with increase in incident irradiance. As observed in Fig. 21a, the net thermal power delivered approaches zero for $R_{wg} < 0.2$ m, due to the greater thermal losses from the receiver in comparison to the irradiation reaching the receiver, which ultimately leads to very high aperture requirements (Fig. 21b). This has a direct consequence on the collection efficiency also, which is analyzed in Fig. 21c. The collection efficiency drastically decreases for smaller radii ($R_{wg} < \sim 0.3$ m). This is attributed to the decrease in net thermal power delivered to the receiver (Fig. 21a) due to increased thermal losses from the receiver. Hence, there is an additional requirement of a minimum waveguide radius to realize high collection efficiencies (Fig. 21c) and low aperture area requirements (Fig. 21b).

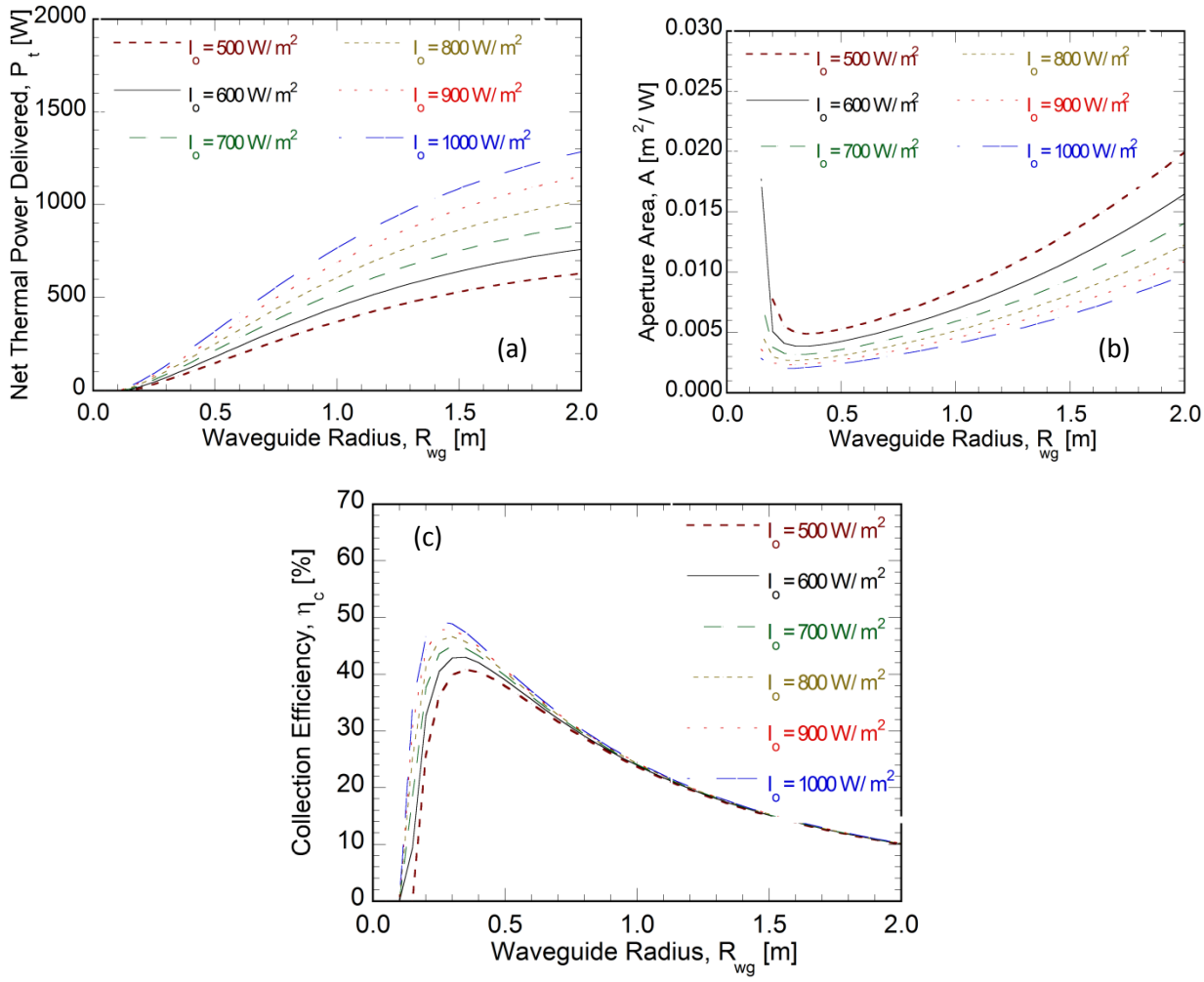

Figure 21. Effects of incident solar irradiance (I_0) and waveguide radius (R_{wg}) on (a) net thermal power delivered, (b) aperture area, and (c) collection efficiency for HTF temperature of T_F = 100 ℃. The values for waveguide thickness (t) and receiver diameter (D_G) are kept constant at 10 mm and 40 mm, respectively.

Figure 22a illustrates the maximum temperature difference between the waveguide made of optical glass ZK7 and ambient (ΔT_{max}) for HTF temperature of 100 ^{0}C and an ambient temperature of T_{amb} = 30 ℃. From known material properties, namely the absorption coefficient and thermal conductivity, the maximum temperature difference depicted in Fig. 22a is obtained as a function of radius and solar irradiation intensity, for a fixed thickness of 10 mm. Figure 22a shows that the maximum temperature difference (ΔT_{max}) increases with increase in incident irradiation intensity. For a given solar irradiance, ΔT_{max} increases and asymptotes to a constant

value with increase in radius due to the exponential attenuation of solar irradiation with increase in path length.

The maximum radius of the waveguide is limited by the critical stress limit which is 8 MPa. Figure 22b shows the variation of stress generated in the waveguide with the waveguide radius and thickness. The stress values increase with an increase in the waveguide radius because of higher temperature rise due to increased absorption in the waveguide. The increase in stress is at a lower rate in waveguides which have greater thickness. This is due to the slower temperature rise in thicker waveguides. Thus, for a given thickness, there is a maximum value up to which the waveguide radius can be increased.

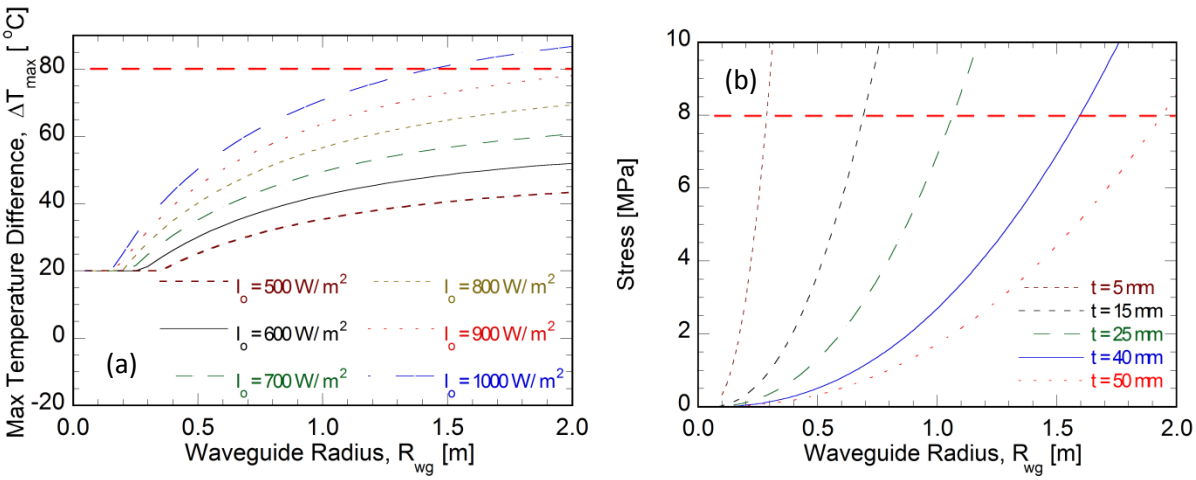

Figure 22. (a) Effects of incident solar irradiance (I_0) and waveguide radius (R_{wg}) on maximum temperature difference between the waveguide and ambient air obtained for HTF temperature of T_F = 100 °C. The values for waveguide thickness (t) and receiver diameter (D_G) are kept constant at 10 mm and 40 mm, respectively. (b) Effect of waveguide radius (R_{wg}) and waveguide thickness (t) on the stress induced in the waveguide for a fixed incident solar irradiance (I_0) of 1000 W/m^2. The red line shows the maximum allowable stress which is 8 MPa.

Figure 23 shows how the maximum waveguide radius varies with variation in thickness and the incident solar irradiation. It is limited by the structural and thermal stresses. The thermally induced stress limits the radius value after a particular thickness and the increases in maximum radius with thickness becomes very slow after that. The maximum radius value is lower in case of higher irradiation value which is due to greater temperature rise which is associated with higher irradiation. The convective heat transfer coefficient also plays an important role in

deciding the maximum radius. Higher convective heat transfer coefficient allows for a larger waveguide as the temperature rise is less in this case.

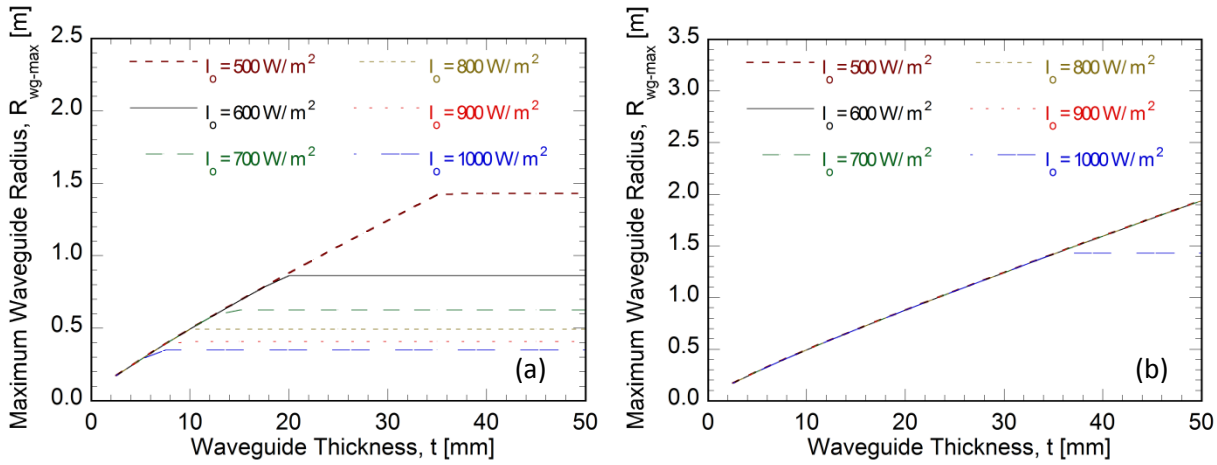

Figure 23. (a) Effects of incident solar irradiance (I_0) and waveguide thickness (t) on the maximum allowable waveguide radius (R_{wg-max}) for (a) when convective heat transfer coefficient (h) is 2.5 W/m^{2}K (b) when convective heat transfer coefficient (h) is 5 W/m^{2}K.

3.7.3 Economic Analysis

Figure 24a shows the cost per unit aperture area (C'') of the radial waveguide concentrator-receiver configuration as a function of radius for various thicknesses. It is observed that the cost per unit aperture area of the radial waveguide concentrator-receiver configuration decreases with increase in radius due to the inverse relation of C'' with Rwg [Eq. (11)], while increasing with thickness due to increase in waveguide material. For a given incident irradiance, the minimum waveguide cost that satisfies both the thermal stress and structural constraints is observed for the maximum permissible waveguide radius, which varies with incident irradiance (I_o), ΔT^*_{max} and waveguide thickness (t).

Figure 24b depicts the variation of minimum waveguide cost per unit aperture area with waveguide thickness and incident irradiation for $\Delta T^*_{max} = 80$ ℃. The corresponding optimal waveguide radius that yields the minimum waveguide cost is shown in Fig. 24c. The optimal waveguide radius that yields the minimum waveguide cost coincides with the maximum permissible waveguide span based on both thermal stress and structural considerations. For a given incident irradiation, the minimum cost initially decreases with increase in thickness, reaches a minimum before increasing with further increase in thickness (Fig. 24b). For smaller

thickness values, the receiver cost component—the first term in Eq. (11)—dominates, and C″ decreases with increase in thickness due to the subsequent increase in optimal radius (Fig. 24c).

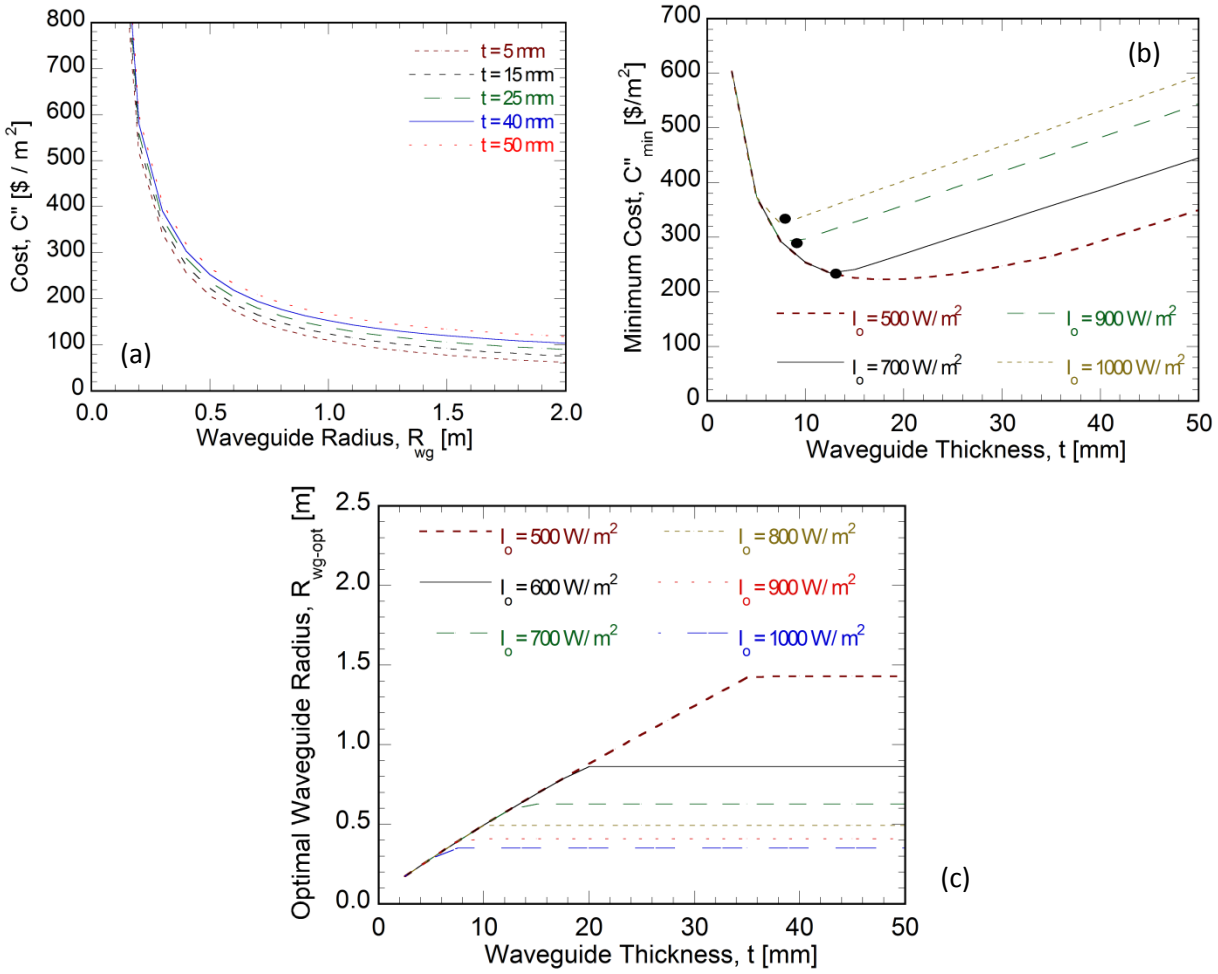

Figure 24. Effects of waveguide thickness and radius on (a) cost per unit aperture area of the radial waveguide concentrator-receiver system. Influence of waveguide thickness and incident irradiation intensity on (b) minimum waveguide-receiver cost per unit aperture area and the corresponding (c) optimal waveguide radius obtained for $\Delta T^{*}_{max} = 80$ ℃.

However, after a certain thickness value, the waveguide cost component—the second term in Eq. (11)—dominates, leading to an increase in the cost per unit aperture area of the receiver-concentrator configuration with increase in thickness. The optimal waveguide thickness that yields the lowest cost of the planar waveguide-receiver configuration is identified by the circular markers for $\Delta T^{*}_{max} = 80$ ℃ in Fig. 24b, which is observed to decrease with increase in incident irradiation intensity. As the irradiance increases, the least cost per unit area is obtained for

thinner waveguides (Fig. 24b) to compensate for the restriction of maximum permissible waveguide radius to lower values (Fig. 24c) based on thermal stress and structural requirements. Therefore, as irradiance increases, the minimum C'' steadily increases due to smaller values of optimal radius [Eq. (11)].

Figure 25a shows the levelized cost of power [Eq. (12)] as functions of thickness and radius for application temperature requirements of 100 ℃, and incident irradiance of 1000 W/m^2. For smaller radius values, the LCOP is high due to low thermal power delivered (Fig. 21a). As the waveguide radius increases, the LCOP decreases due to the increase in thermal power delivered (Fig. 21a). With further increase in waveguide radius, the LCOP reaches a minimum (Fig. 25a) and then increases again due to the increase in cost [Eq. (12)], while the net thermal power delivered levels off (Fig. 21a). In Fig. 14a, it is also observed that the LCOP increases with increase in thickness due to the corresponding increase in cost with increase in material weight content of waveguide [Eq. (12)]. Figure 25b shows the LCOP as a function of radius and incident irradiance for a fixed thickness of 5 mm. It is seen that the LCOP increases significantly with a decrease in incident irradiance due to the decrease in thermal power delivered (Fig. 21a).

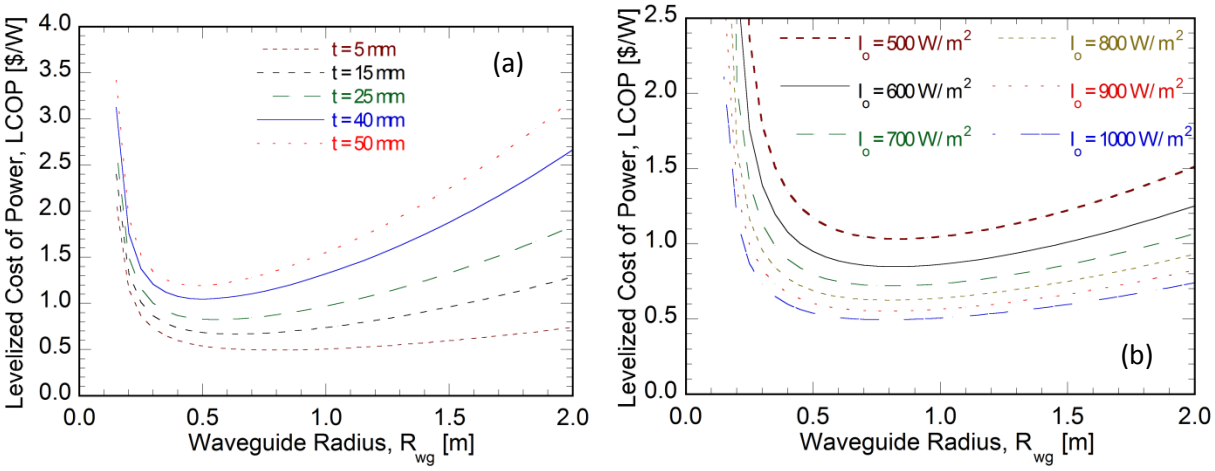

Figure 25. (a) Effect of waveguide thickness and radius on levelized cost of power. (b) Effect of waveguide radius and incident irradiance values (I_0) on levelized cost of power.

The values of radius and thickness that minimize the LCOP, while also satisfying the design constraints based on thermal and structural stress considerations, have been presented in Table 2. The optimal waveguide configuration that yields the least LCOP for different incident irradiance (pertaining to different geographical conditions) and convective heat transfer coefficients is

presented in the table. The application temperature requirements of $T_F = 100$ ℃ corresponds to low temperature desalination [52]. The corresponding waveguide-receiver cost in \$/m^2, aperture area required per unit thermal power delivered in m^2/W and collection efficiency are also shown in Table 2. The optimal waveguide concentrator configurations identified also satisfy the design requirements based on thermal and structural stress constraints.

Table 2. Preferred planar waveguide design based on minimum LCOP for $\Delta T^*_{max} = 80$ ℃. The minimum values of the objective function are italicized and listed in bold face.

Incident Irradiance, I_0 [W/m^2]	Radius, R_{wg} [m]	Thickness, t [mm]	Cost, C'' [\$/m^2]	Levelized Cost of Power LCOP, [\$/W]	Aperture Area, A [m^2/W]	Collection Efficiency, η_C [%]
A. Low temperature thermal desalination ($T_F = 100$ ℃)						
600	0.5	10	252.09	***1.077***	0.0043	39.01
800	0.5	10	252.09	***0.781***	0.0031	40.35
1000	0.5	10	252.09	***0.612***	0.0024	41.16
B. High temperature CST power generation ($T_F = 400$ ℃)						
600	0.6	12.5	233.23	***1.481***	0.0063	26.25
800	0.6	12.5	233.23	***0.988***	0.0042	29.51
1000	0.6	12.5	233.23	***0.741***	0.0032	31.46

It can be seen from Fig. 26a that the minimum LCOP decreases with increase in irradiance due to the increase in net thermal power delivered, and correspondingly, the aperture area requirement also decreases. The optimal waveguide radius increases with increase in thickness up to a point and then starts decreasing. This is due to the stress constraints. The optimal radius is lower for higher incident irradiance. These trends can be seen in Fig. 26b. Fig. 26c shows the effect of convective heat transfer coefficient on the minimum LCOP. The minimum LCOP value reaches its lowest value at a smaller thickness for h = 2.5 W/m^{2}K when compared to h = 5 W/m^{2}K.

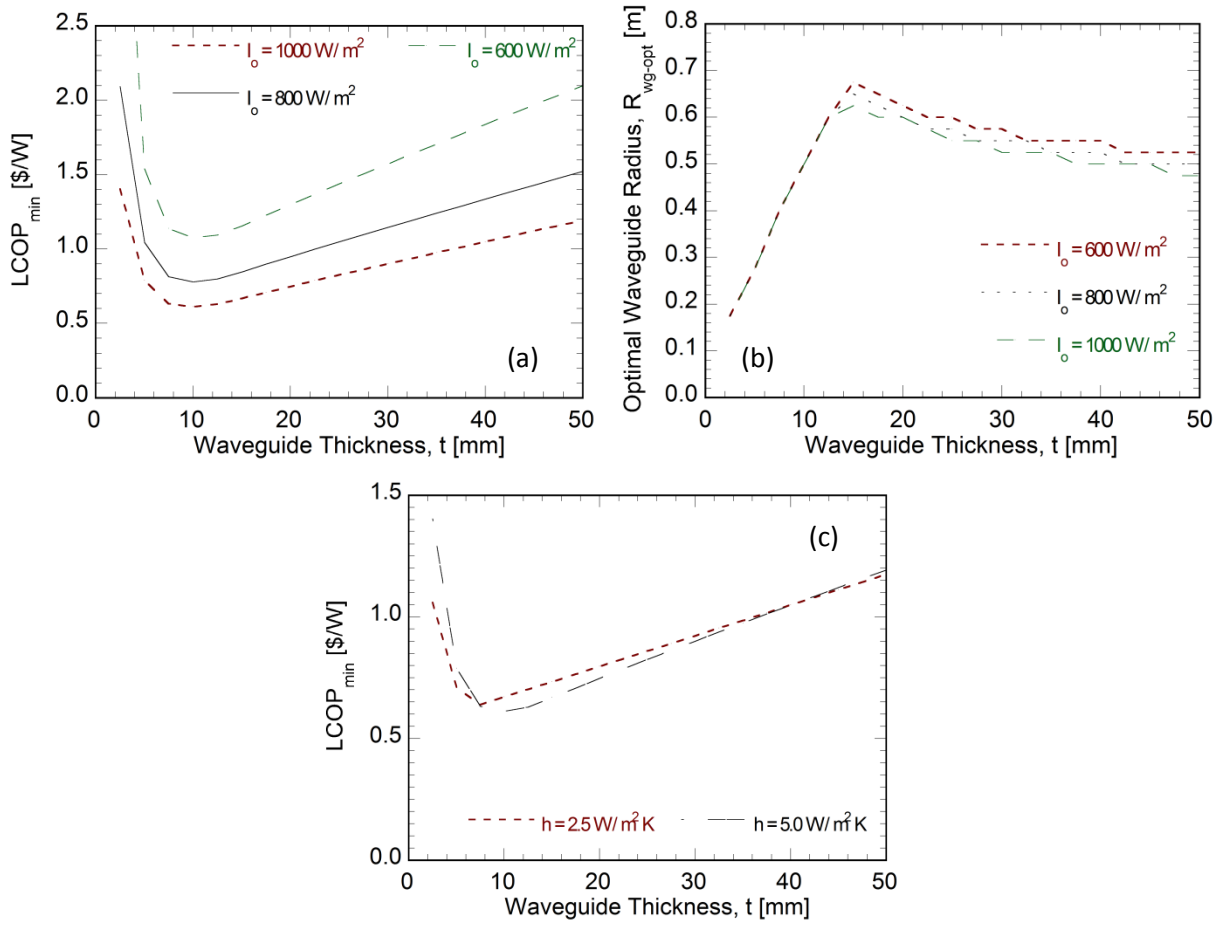

Figure 26. Effect of waveguide thickness and incident irradiance values (I_0) on (a) levelized cost of power and (b) optimal waveguide radius. (c) Effect of waveguide thickness and convective heat transfer coefficient (h) on levelized cost of power.

In general, for $\Delta T^*_{max} = 80$ ℃, the optimal design configuration with least LCOP is obtained for R_{wg} = 0.5 m and t = 10 mm for different irradiance values for low temperature applications and R_{wg} = 0.6 m and t = 12.5 mm for high temperature applications (Table 2) and the corresponding cost per unit area is 252 $/m2 for low temperature applications and 233 $/m2 for high temperature applications. The least LCOP decreases with increase in irradiance due to the increase in net thermal power delivered, and correspondingly, the aperture area requirement also decreases. Comparing Tables 2A and B, the least LCOP increases with increase in application temperature requirements due to increased thermal losses at the receiver that reduce the net thermal power delivered. For instance, the least LCOP obtained for $I_0 = 1000\ W/m^2$ increases from 0.612 $/W for T_F = 100 ℃ (Table 2A) to 0.741 $/W for T_F = 400 ℃ (Table 2B).

Concomitantly, the aperture area requirement also increases and the collection efficiency is observed to decrease. Overall, the planar waveguide design configuration with the least LCOP, smallest aperture area requirement and highest collection efficiency is obtained for applications that require low temperature and regions with high incident irradiance (Table 2).

3.8. Conclusions

An analytical closed-form solution was developed for the coupled optical and thermal transport of incident solar irradiation within a radial planar waveguide concentrator integrated to a central receiver. A systematic parametric study was conducted to establish the relationship between the various design and operating parameters on the system performance which is quantified in terms of net thermal power delivered to the receiver from the waveguide, collection efficiency and aperture area requirement.

The utility of results in guiding practical designs was demonstrated for a planar waveguide concentrator made of optical ZK7 glass. Feasible design and operational envelopes of the radial planar waveguide concentrator-receiver system are reported based on the structural (wind loading) and thermal (thermal stress, and maximum continuous operation temperature limit) constraints.

The results from the analytical model are backed up by the TracePro simulations. Parametric study is conducted using the ray trace software which gives clear trends about how the energy collected, collection efficiency, absorption and decoupling loss depend on the parameters like waveguide thickness, waveguide radius, receiver radius and the grating size.

A simple cost analysis was also developed and the preferred design configurations within the feasible regime that minimize the LCOP ($/W) of the disruptive, planar waveguide solar thermal concentrator for two example applications of low temperature desalination and concentrated solar thermal power generation are reported in Table 2.

Chapter 4. Conclusions and Future Work

The performance of the air-cooled air gap membrane distillation system is comparable to the water-cooled systems even though it has lower energy requirements. The modular design which has been proposed here helps in increasing the capacity of the system by adding more modules, when required. It also helps in better utilization of the thermal energy of the heated saline water by passing the water through multiple passes till the temperature of the water decreases to a point where it is not suitable for the process. The superhydrophobic surface helps in improving the flux. It also reduces the temperature drop for the saline water as it passes through the channel.

Of the parameters which were studied, the conductivity of the support mesh had a significant effect on the yield from the setup. The copper mesh which has a conductivity of about 401 W/mK resulted in the highest flux values followed by the Aluminum mesh and steel mesh. The plastic mesh resulted in about 30% lesser flux values. Increasing the air gap resulted in lower flux values. In series configuration, the hydrophobic surface with the small air gap works best and results in about three times more yield when compared to the single pass water-cooled system.

Further studies should be conducted to model and improve the yields for the air-cooled AGMD module. Long term performance of the module in natural environment where it is cooled by the ambient air should be studied. Effect of the structure of the saline channel on the yield can also be studied. Dimensionless form of the results should also be looked at in future. Using regression analysis on the collected data, equations can be developed which predict the flux values at different values of air gap, conductivity of mesh and saline feed temperature.

To make the desalination process fully sustainable, it is proposed that a solar energy concentration system be used to meet the thermal needs of the desalination system. Thus, an analytical model for a radial waveguide based solar concentration system was developed. An analytical closed-form solution for the waveguide was developed for the coupled optical and thermal transport of incident solar irradiation within a radial planar waveguide concentrator integrated to a central receiver. A systematic parametric study was conducted to establish the relationship between the various design and operating parameters on the system performance which is quantified in terms of net thermal power delivered to the receiver from the waveguide, collection efficiency and aperture area requirement.

Feasible design and operational limits for the radial planar waveguide concentrator-receiver system are reported based on the structural and thermal (thermal stress, and maximum continuous operation temperature limit) constraints.

A separate parametric study is conducted using the ray trace software which gives clear trends about how the energy collected, collection efficiency, absorption and decoupling loss depend on the parameters like waveguide thickness, waveguide radius, receiver radius and the grating size.

A cost model was also developed and the preferred design configurations that minimize the levelized cost of power ($/W) of the radial planar waveguide solar thermal concentrator for both low and high temperature applications are reported.

In future, endeavors should be made to manufacture the proposed radial waveguide and pair it initially with the AGMD module and later use it in other low and high temperature applications. A multi-variable optimization analysis using an optimization algorithm can be conducted for the different dimensions of the radial waveguide and the lens array. Studies should also be conducted to develop passive tracking techniques and apply it to this system. Other materials which have lower absorption coefficients and higher working temperature can also be explored to improve the collection efficiency of the system and decreases the LCOP.